

## A DNS BASED ANALYSIS OF NOISE GENERATION BY A TURBULENT PREMIXED FLAME

**Ali Haghiri, Mohsen Talei\*, Michael J. Brear**  
 Department of Mechanical Engineering,  
 University of Melbourne, VIC 3010, Australia.  
 \*mohsen.talei@unimelb.edu.au

**Evatt R. Hawkes**  
 School of Photovoltaic and Renewable Energy Engineering /  
 School of Mechanical and Manufacturing Engineering,  
 University of New South Wales, Sydney 2052, Australia.

### ABSTRACT

Direct numerical simulation (DNS) is used to study sound generation by an unconfined, turbulent premixed flame. The computational grid is set up such that both the near and far fields are fully resolved, and simple chemistry is used to reduce the computational cost. In keeping with earlier, simpler studies by the group, flame annihilation events are again observed as strong monopolar sources of sound, and their amplitudes are consistent with the groups previously published scalings. Analysis of the radiated sound then shows broadband spectra, with the observed frequency of peak amplitude being consistent with those observed experimentally by others.

### INTRODUCTION

Combustion-generated noise is unwelcome in many applications across the transport, power generation and industrial sectors. In particular, combustion-generated noise is becoming a major noise source in aeroengines. This is due to considerable advances over the last decades in reducing the noise from other sources such as fan and jet noise (Dowling & Mahmoudi (2015); Duran *et al.* (2014)).

Combustion-generated sound has an additional importance because it hampers development of low-emission, premixed combustors. These types of combustors are susceptible to so called ‘thermoacoustic instability’ associated with the sound generated by the flame inside the combustor. The interaction of the reflected acoustic waves from the combustor’s walls and nozzle with the flame can trigger instability and produce strong pressure fluctuations, leading to engine failure in extreme cases.

Review of our current understanding of sound generation by open turbulent flames shows that combustion noise sources are considered to be a distribution of monopolar sound sources with different strengths and frequencies (Bragg (1963); Smith & Kilham (1963); Rajaram *et al.* (2006); Rajaram & Lieuwen (2009); Dowling & Mahmoudi (2015)). Many studies (e.g. Hurle *et al.* (1968); Strahle (1978)) have argued that the fluctuating heat release rate is the dominant source of noise in flames. In a number of one- (1D) and two-dimensional (2D) numerical studies (Jiménez

*et al.* (2015); Talei *et al.* (2014, 2012a,b, 2011)), destruction of the flame surface area (known as ‘flame annihilation’) has been shown to have a significant contribution to the rate of change of heat release rate, and therefore the generated sound in laminar premixed flames. However, it is unclear whether these events are also significant sources of noise in turbulent premixed flames.

Direct numerical simulation (DNS) is a means to gain an improved understanding of the sound generation mechanisms since all relevant flow physics are resolved. However, DNS is computationally very expensive, in particular for aeroacoustic simulations of combustions flows. This is because both the flame and the far field need to be fully resolved in these simulations. Due to this limitation, and to the best of our knowledge, DNS of sound generation by a turbulent premixed flame has not been attempted in the literature.

This paper therefore presents a DNS of sound generation by a turbulent premixed flame. By resolving both the flame and the radiated sound, the acoustic sources can be investigated directly using these simulations. A special focus of this paper is the sound generated by the observed flame annihilation events. The spectral content of the radiated sound is then examined and compared briefly to experiments performed by others.

### GOVERNING EQUATIONS

Using a single-step, irreversible chemical reaction, the governing equations for the conservation of mass, momentum, total energy, and deficient reactant species mass fraction are respectively as follows:

$$\frac{\partial \rho}{\partial t} + \frac{\partial \rho u_i}{\partial x_i} = 0, \quad (1)$$

$$\frac{\partial \rho u_j}{\partial t} + \frac{\partial \rho u_i u_j}{\partial x_i} = -\frac{\partial p}{\partial x_j} + \frac{\partial \tau_{ij}}{\partial x_i}, \quad (2)$$

$$\frac{\partial \rho E_t}{\partial t} + \frac{\partial u_j (\rho E_t + p)}{\partial x_j} = \frac{\partial u_i \tau_{ij}}{\partial x_j} - \frac{\partial q_j}{\partial x_j}, \quad (3)$$

and

$$\frac{\partial \rho Y_F}{\partial t} + \frac{\partial \rho u_j Y_F}{\partial x_j} = \frac{\partial}{\partial x_j} \left( \rho D \frac{\partial Y_F}{\partial x_j} \right) - \dot{\omega}_F, \quad (4)$$

where  $x$  and  $t$  are the spatial coordinate and time respectively. In addition,  $\rho$  is the mixture density,  $u_j$  is the  $j$ -component of velocity,  $Y_F$  is the fuel mass fraction (progress variable),  $p$  is the pressure,  $E_t$  is the total energy per unit mass (including sensible, kinetic, and chemical energy),  $q_j$  is the heat flux vector, and  $\tau_{ij}$  is the  $ij$ -component of the viscous stress tensor. The quantities  $E_t$ ,  $q_j$  (assuming constant heat capacity),  $\tau_{ij}$  and  $p$  are given by,

$$E_t = \frac{p}{\rho(\gamma-1)} + \frac{1}{2} u_i u_i + Y_F Q, \quad (5)$$

$$q_j = -\lambda \frac{\partial T}{\partial x_j} - \sum_{k=1}^{N_s} \left( h_k^0 \rho D \frac{\partial Y_k}{\partial x_j} \right), \quad (6)$$

$$\tau_{ij} = \mu \left[ \frac{\partial u_i}{\partial x_j} + \frac{\partial u_j}{\partial x_i} - \frac{2}{3} \frac{\partial u_k}{\partial x_k} \delta_{ij} \right], \quad (7)$$

and

$$p = \rho R T \sum_{k=1}^{N_s} \frac{Y_k}{M_k} = \rho \left( \frac{R}{M} \right) T, \quad (8)$$

where  $\gamma$  is the heat capacity ratio,  $Q$  is the heat of reaction per unit mass of reactant,  $h_k^0$  is the chemical enthalpy of formation of species  $k$  evaluated at a reference temperature  $T_{ref}$ ,  $\mu$  is the dynamic viscosity,  $D$  is the binary mass diffusion coefficient,  $\lambda$  is the mixture thermal conductivity,  $R$  is the ideal gas constant,  $M_k$  is the species molecular weight,  $M$  is the mixture molecular weight, and  $\delta_{ij}$  is the Kronecker delta. The variation of  $\mu$  with temperature is modelled using a power-law,

$$\mu = \mu_{ref} \left( \frac{T}{T_{ref}} \right)^{0.76}, \quad (9)$$

where  $\mu_{ref}$  is the fresh gas absolute viscosity. The fuel species reaction rate  $\dot{\omega}_F$  may be obtained using the Arrhenius law,

$$\dot{\omega}_F = \Lambda \rho Y_F \exp \left[ -\frac{\beta(1-\theta)}{1-\alpha(1-\theta)} \right], \quad (10)$$

where

$$\Lambda = B \exp \left( -\frac{\beta}{\alpha} \right), \quad \theta = \frac{T - T_u}{T_f - T_u}, \quad (11)$$

$$\alpha = \frac{T_f - T_u}{T_f}, \text{ and } \beta = \frac{E_a(T_f - T_u)}{R T_f^2}. \quad (12)$$

Note that  $B$  is the pre-exponential factor,  $\beta$  is the Zel'dovich number,  $T_f$  is the adiabatic flame temperature,  $T_u$  is the fresh (unburned) mixture temperature,  $E_a$  is the activation energy and  $\alpha$  is the heat release parameter.

## Non-dimensional Variables

The following non-dimensional variables are defined:

$$\text{Re}_{ac} = \left( \frac{aL}{\nu} \right)_{ref}, \quad \text{Pr} = \left( \frac{\nu}{D_{th}} \right)_{ref},$$

$$\text{Le} = \left( \frac{D_{th}}{D} \right)_{ref}, \quad \text{and } \text{Da} = \left( \frac{\Lambda L}{a} \right)_{ref}. \quad (13)$$

Note that  $a$  is the sonic velocity,  $L_{ref}$  is the reference length which is equal to the jet diameter  $D$ ,  $\text{Re}_{ac}$  is the acoustic Reynolds number,  $\text{Pr}$  is the Prandtl number,  $\text{Le}$  is the fuel Lewis number,  $\text{Da}$  is the Damköhler number,  $D_{th}$  is the thermal diffusivity coefficient, and  $\nu$  is the kinematic viscosity.

## NUMERICAL METHOD AND FLOW CONFIGURATION

The governing equations (1-4) are solved using a modified version of the numerical solver S3D (Chen *et al.* (2009)) known as S3D-SC (Karami *et al.* (2012, 2015)). The solver features an 8<sup>th</sup> order central differencing scheme for spatial derivatives, combined with a 6-stage, 4<sup>th</sup> order explicit Runge–Kutta time integrator. It is fully parallelised using the MPI implementation. To suppress numerical noise at high wave numbers, a 10th-order filter is applied every 10 time steps. The computational domain is decomposed into a 3D structured Cartesian mesh. The boundary conditions

Table 1: Simulation parameters.

Jet diameter	D
Domain size	15D × 16D × 16D
Grid resolution	1800 × 800 × 800
Mean inlet jet Mach number	0.4
co-flow Mach number	0.004
Non-dim. fresh mixture temperature	2.5
Heat release parameter ( $\alpha$ )	3
Jet Reynolds number (Re)	4000
Inlet turbulence intensity ( $u'/\bar{U}_j$ )	0.1
$\delta_{in}/D$	0.07
$S_L/a_{ref}$	0.007
$\beta$	8.0
Da	19.44
Pr	0.75
Le	1.0

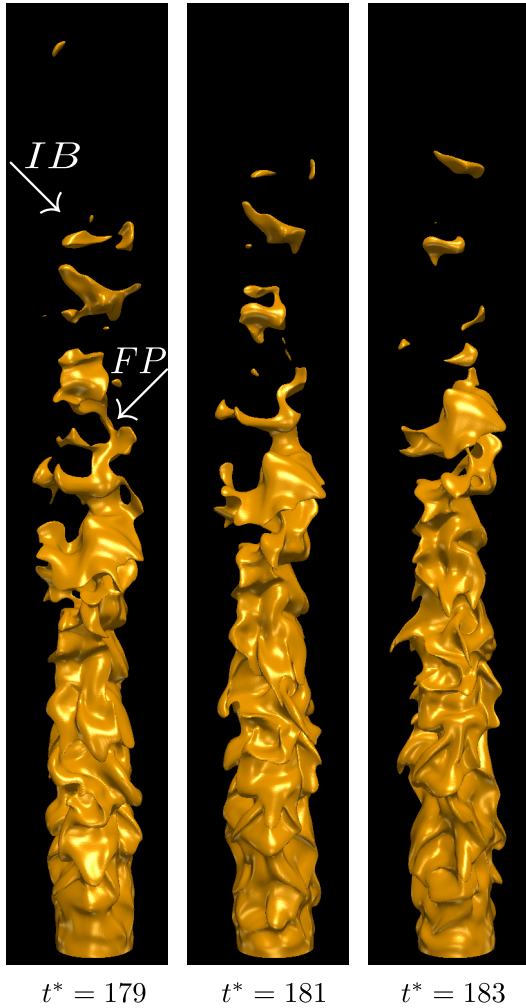


Figure 1: Several instantaneous iso-surfaces of the progress variable  $Y_F = 0.37$ . FP: ‘flame pinch-off’ event; IB: ‘flame island burn-out’ event.

are implemented based on 3D Navier-Stokes Characteristic Boundary Condition (3DNSCBC) (Yoo & Im (2007)). All non-reflecting outflow boundaries are carefully treated to avoid spurious noise reflections.

A subsonic round jet of unburned premixed mixture (reactant) is injected into an open, hot environment of adiabatic combustion products. The environment temperature is equal to the product temperature. A coflow with a low velocity (1% of the jet mean velocity) surrounds the jet flame at the burned mixture’s temperature to mimic natural convection around jet flames in real conditions. A velocity fluctuation,  $u'$ , is imposed on the mean inlet velocity field using an auxiliary homogeneous isotropic turbulence obtained based on the Passot-Pouquet energy spectrum (Passot & Pouquet (1987)). This frozen turbulence field is added to the domain using the Taylor hypothesis. The computational, flow and flame parameters are summarised in Table 1.

A uniform grid with a resolution of  $8.250 \times 10^{-3}D$  is setup in the streamwise direction ( $x/D$ ). While maintaining a uniform grid spacing of  $8.250 \times 10^{-3}D$  for  $6 \leq |y/D| \leq 10$  and  $6 \leq |z/D| \leq 10$ , an algebraically stretched mesh with a stretching ratio of less than 2.5% is used in the transverse directions ( $y/D$  and  $z/D$ ). Care was taken to ensure adequate

resolution of the flame by having at least 8 grid points inside the flame thickness at all times. Moreover, the computational domain was long enough to properly capture the acoustic waves produced by the flame.

Based on the prescribed inlet jet velocity and the streamwise domain length, a jet flow-through time is defined as  $\tau_j = L_x/U_j$ . The simulation was performed using a constant time step for  $10\tau_j$  to provide a statistically stationary solution. The simulation required approximately 1,000,000 CPU-hours running on 7680 CPUs (Intel Xeon Sandy Bridge technology, 2.6 GHz) for 130 hours.

## RESULTS AND DISCUSSION

This section is organised as follows. Different types of flame annihilation events are visually examined first. Next, the acoustic field is examined to investigate the effect of the flame annihilation events on the produced sound. Then, the pressure fluctuations at a given location in the acoustic field are compared with those produced by annihilation of simple flame geometries. Finally, a spectral analysis of the radiated sound to the far field is performed and compared with an existing correlation obtained from experimental studies.

### Flame Annihilation Events

Several instantaneous snapshots of the progress variable  $Y_F = 0.37$  iso-surface are shown in figure 1. This iso-level is selected such that the corresponding progress variable is close to the point of peak heat release in a one-dimensional laminar premixed flame with the same chemistry model. In the downstream region near the flame tip, rapid flame annihilation events are observed to occur. Two interesting geometries of these events which result in topological changes are specifically noted. The first type is called a ‘flame pinch-off’(FP) event, in which a single flame surface breaks into two surfaces. This collision creates pockets of unburned gases which are consumed as they travel downstream. We refer to this phenomenon as ‘flame island burn-out’ (IB).

### Flame-Generated Noise

To examine the role of annihilation events in the overall sound produced by the flame, several snapshots of the dimensionless dilatation field  $(D/a_{ref})\nabla \cdot \vec{u}$  extracted at the

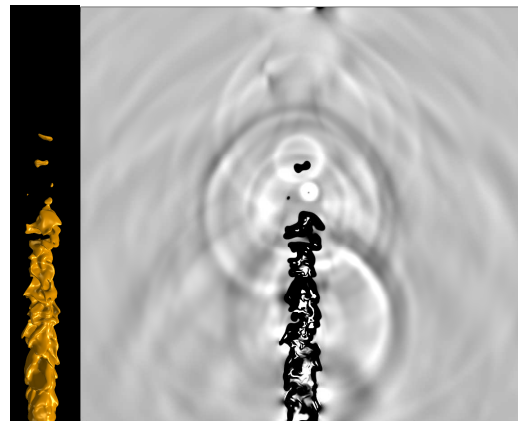


Figure 2: A slice of the dimensionless dilatation field  $(L_{ref}/a_{ref})\nabla \cdot \vec{u}$  located at the centre of the jet.

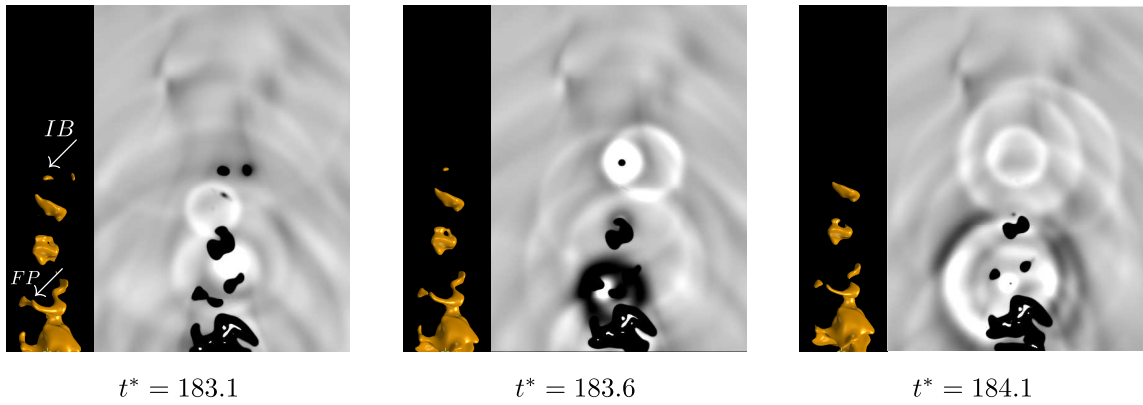


Figure 3: The dimensionless dilatation field  $(D/a_{ref})\nabla\cdot\bar{u}$  for several instants close to the flame tip.

central plane through the jet are shown in figure 2. The first striking observation is that the acoustic field features discrete monopolar sound sources. The sound produced from these sources, originating some distance downstream of the nozzle, clearly dominate the incoming noise at the inflow. It should be noted that the presence of a monopolar acoustic field in a premixed flame has also been confirmed extensively in the literature (e.g. Bragg (1963) and Smith & Kilham (1963)). The present study clearly shows the significant contribution from the annihilation events to this observed behaviour.

Figure 3 shows the dilatation field for several instants close to the flame tip. As can be seen, the two annihilation events labelled IB and FP produce monopolar acoustic waves. Our previous studies (Talei *et al.* (2014, 2012a,b, 2011)) showed that such annihilation events are significant sound sources in acoustically excited laminar premixed flames. This conclusion also appears to be valid for the turbulent flame studied in this paper. However, a more detailed analysis is required to quantify the contribution of flame annihilation to the overall radiated sound.

### Noise Generation by Annihilation Events in Simple Geometries

The aim of this section is to compare the sound produced by a typical annihilation event in the flame with that produced with annihilation events by simple geometries. Two types of annihilation events are considered: axisymmetric and spherically symmetric annihilation events. The simulations for these simple geometries are setup with the same flame parameters as the turbulent flame. After

initialising the flow field, the spherical and cylindrical premixed flames start to propagate towards the origin and produce sound after they annihilate.

Figure 4 shows a comparison between the noise produced by the two simple flame topologies and a typical annihilation event in the turbulent flame at some distance from the centre of these pockets. As can be seen, the magnitude of the pressure fluctuations in the turbulent flame lies between those in the spherical and cylindrical flame annihilation events. It should be noted that the peak pressure observed in figure 4c originates from the ‘flame pinch-off’ event marked as FP in figure 3. This indicates that the ‘flame pinch-off’ event can be perhaps modelled approximately by a collapsing cylindrical flame.

### Spectral Analysis

The frequency spectrum of the produced sound is calculated at two different planes perpendicular to the jet axis with the axial positions of  $H/D = 3.75$  and  $7.5$ . Eight uniformly-distributed virtual microphones at  $r/D = 6$  are placed on each plane to measure the sound intensity (see figure 5). The mean frequency spectrum is then obtained by averaging the spectrum of all individual microphones. To reduce the so-called ‘spectral leakage’, a Hanning window technique (Rajaram *et al.* (2006); Rajaram & Lieuwen (2009); Bui *et al.* (2008)) was used to perform the fast Fourier transform (FFT) of each time signal at each probe.

The averaged calculated spectra at each plane are shown in figure 6. Similar to the observations in earlier experimental studies (e.g. Rajaram *et al.* (2006); Rajaram & Lieuwen (2009)), the produced sound is found to be broad-

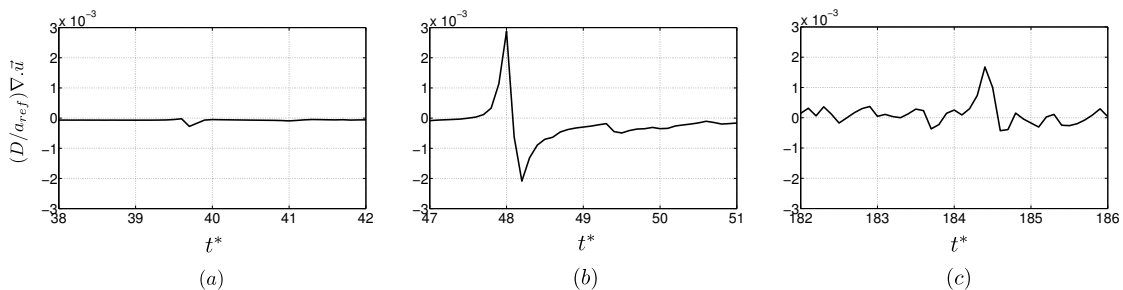


Figure 4: Fluctuations of the dilatation produced by a) spherical flame, b) cylindrical flame and c) turbulent premixed flame.

band in nature in our study.

Rajaram *et al.* (2006) and Rajaram & Lieuwen (2009) investigated noise generation by a number of turbulent premixed flames and found that the frequency of peak emissions  $f_{peak}$  across all burners, flow velocities, fuel/air ratios, and fuel types, is mainly a function of the averaged flame length and mean inlet velocity. They showed that the peak Strouhal number ( $St=f_{peak}L/U_j$ ) is in the range of 0.6 to 1.9. In order to calculate the peak Strouhal number for the present simulation, the averaged flame length needs to be calculated. For this end, the time-averaged temperature and reaction rate fields are first obtained (see figure 7). As can be seen, the flame length is approximately equal to  $8.2D$ . Using this value for the averaged flame length, the peak Strouhal numbers at the two axial observer positions are equal to 1.2 and 1.7, respectively. These values therefore lie within the range of the peak Strouhal numbers found experimentally by Rajaram *et al.* (2006) and Rajaram & Lieuwen (2009).

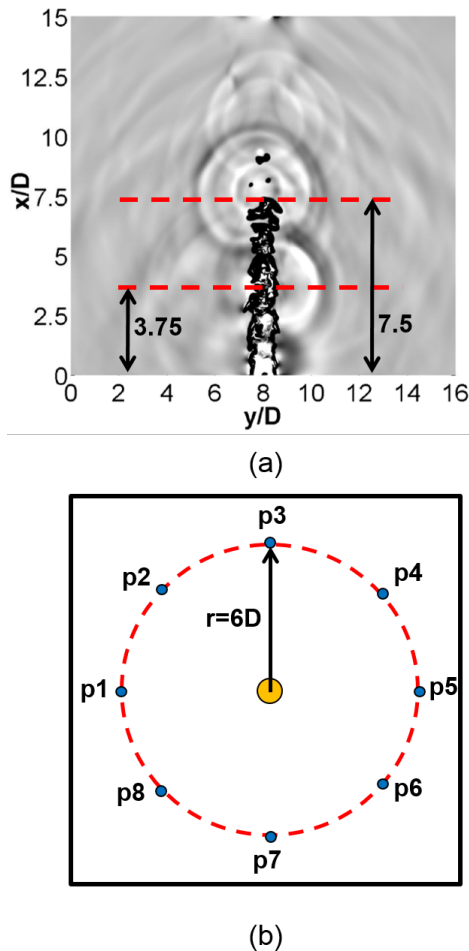


Figure 5: The locations of eight uniformly-distributed virtual microphones at two different axial observer positions ( $H/D = 3.75$  and  $7.5$ ) with a radial distance from the flame centreline ( $r/D = 6$ ): a) front view and b) top view.

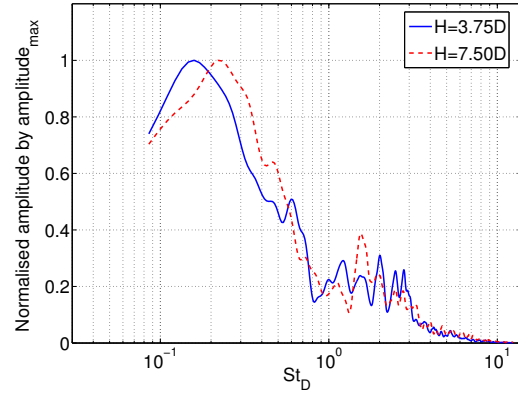


Figure 6: Calculated noise spectra at two different axial observer positions.

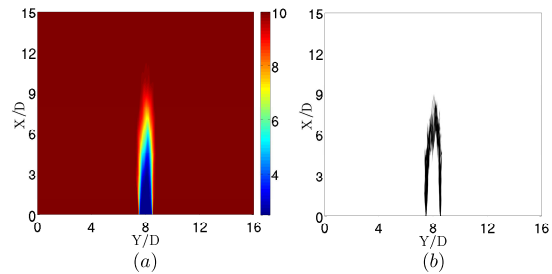


Figure 7: Time-averaged non-dimensional temperature (a) and reaction rate (b) fields at the jet's centreline plane.

## CONCLUSIONS

A numerical study of sound generation by a turbulent premixed flame was performed using direct numerical simulation (DNS). Since both the flame (near) and the acoustic (far) fields needed to be fully resolved, single-step chemistry was used to reduce the computational cost of these large simulations. Also, three dimensional Navier-Stokes Characteristic Boundary Conditions (3DNSCBC) were used at the outflow boundaries to avoid spurious reflections. The simulation was performed for ten jet-flow-through times to approximate a statistically stationary solution and to obtain a large enough dataset for analysing the spectral content of the noise produced.

The iso-surfaces of a specific reaction progress variable were first examined, and two types of flame annihilation event were identified. These were termed 'flame pinch-off', in which a single flame surface breaks into two surfaces, and 'flame island burn-out', in which isolated pockets of unburned gases are consumed. The acoustics of these two forms of annihilation events have been examined in earlier, simpler studies by the group in 1D and 2D problems. These annihilation events were again found to produce monopolar sound in the present study, with amplitudes that are consistent with the group's previously published scalings.

The spectra of the radiated noise were then examined. These were found to be broadband in nature, with a peak amplitude scaling that was consistent with experimental studies published by others. Ongoing work is now examining the contribution of the flame annihilation events to the

overall radiated sound.

## ACKNOWLEDGEMENTS

This study was supported by the Advanced Centre for Automotive Research and Testing (ACART, www.acart.com.au), the Australian Research Council (ARC) and the National Computational Merit Allocation Scheme, supported by the Australian Government. The computational facilities supporting this project included the Australian National Facility (NCI), the partner share of the NCI facility provided by Intersect Australia Pty Ltd., the Peak Computing Facility of the Victorian Life Sciences Computation Initiative (VLSCI) and iVEC (Western Australia).

## REFERENCES

- Bragg, S. L. 1963 Combustion noise. *Journal of the Institute of Fuel* **36** (1), 12–16.
- Bui, T. P., Schröder, W. & Meinke, M. 2008 Numerical analysis of the acoustic field of reacting flows via acoustic perturbation equations. *Computers & Fluids* **37** (9), 1157–1169.
- Chen, J. H., Choudhary, A., De Supinski, B., DeVries, M., Hawkes, E. R., Klasky, S., Liao, W. K., Ma, K. L., Mellor-Crummey, J., Podhorszki, N., Sankaran, R., Shende, S. & Yoo, C. S. 2009 Terascale direct numerical simulations of turbulent combustion using s3d. *Computational Science & Discovery* **2** (1), 015001.
- Dowling, A. P. & Mahmoudi, Y. 2015 Combustion noise. *Proceedings of the Combustion Institute* **35**, 65–100.
- Duran, I., Moreau, S., Nicoud, F., Livebardon, T., Bouty, E. & Poinsot, T. 2014 Combustion noise in modern aero-engines. *Journal of Aerospace Lab* **7**, 1–11.
- Hurle, I. R., Price, R. B., Sugden, T. M. & Thomas, A. 1968 Sound emission from open turbulent premixed flames. *Proceedings of the Royal Society of London A* **303** (1475), 409–427.
- Jiménez, C., Haghiri, A., Talei, M., Brear, M. J. & Hawkes, E. R. 2015 Sound generation by premixed flame annihilation with full and simple chemistry. *Proceedings of the Combustion Institute* **35**, 3317–3325.
- Karami, S., Hawkes, E. R. & Talei, M. 2012 A direct numerical simulation study of a turbulent lifted flame in hot oxidizer. In *18th Australasian Fluid Mechanics Conference Launceston, Australia*, pp. 8–11.
- Karami, S., Hawkes, E. R., Talei, M. & Chen, J. H. 2015 Edge flame dynamics in a turbulent lifted jet flame. *Proceedings of the 2014 Summer Program, Center for Turbulence Research (Stanford, CA)* pp. 137–146.
- Passot, T. & Pouquet, A. 1987 Numerical simulation of compressible homogeneous flows in the turbulent regime. *Journal of Fluid Mechanics* **181**, 441–466.
- Rajaram, R., Gray, J. & Lieuwen, T. 2006 Premixed combustion noise scaling: Total power and spectra. *AIAA Paper* **2612**.
- Rajaram, R. & Lieuwen, T. 2009 Acoustic radiation from turbulent premixed flames. *Journal of Fluid Mechanics* **637**, 357–385.
- Smith, T. J. B. & Kilham, J. K. 1963 Noise generation by open turbulent flames. *The Journal of the Acoustical Society of America* **35**, 715.
- Strahle, W. C. 1978 Combustion noise. *Progress in Energy and Combustion Science* **4** (3), 157 – 176.
- Talei, M., Brear, M. J. & Hawkes, E. R. 2011 Sound generation by laminar premixed flame annihilation. *Journal of Fluid Mechanics* **679**, 194–218.
- Talei, M., Brear, M. J. & Hawkes, E. R. 2012a A parametric study of sound generation by premixed laminar flame annihilation. *Combustion and Flame* **159** (2), 757 – 769.
- Talei, M., Brear, M. J. & Hawkes, E. R. 2014 A comparative study of sound generation by laminar, combusting and non-combusting jet flows. *Theoretical and Computational Fluid Dynamics* **28** (4), 385–408.
- Talei, M., Hawkes, E. R. & Brear, M. J. 2012b A direct numerical simulation study of frequency and Lewis number effects on sound generation by two-dimensional forced laminar premixed flames. *Proceedings of the Combustion Institute* **34**, 1093–1100.
- Yoo, C. S. & Im, H. G. 2007 Characteristic boundary conditions for simulations of compressible reacting flows with multi-dimensional, viscous and reaction effects. *Combustion Theory and Modelling* **11** (2), 259–286.